Regulation of phagocytosis in Dictyostelium by the inositol 5-phosphatase OCRL homolog Dd5P4

Loovers, H.M.; Kortholt, A.; de Groote, H.; Whitty, L.; Nussbaum, R.L.; van Haastert, P. J. M.

Published in:
Traffic

DOI:
10.1111/j.1600-0854.2007.00546.x

Publication date:
2007

Traffic 2007; **8:** 618–628
Blackwell Munksgaard

doi: 10.1111/j.1600-0854.2007.00546.x

Regulation of Phagocytosis in *Dictyostelium* by the Inositol 5-Phosphatase OCRL Homolog Dd5P4

Harriët M. Loovers[1,2], Arjan Kortholt[1], Hendrie de Groote[1], Leslie Whitty[3], Robert L. Nussbaum[3] and Peter J. M. van Haastert[1,*]

[1]*Department of Molecular Cell Biology, University of Groningen, Kerklaan 30, 9751NN Haren, The Netherlands*
[2]*Current address: Department of Biology, National University of Ireland Maynooth, Maynooth, Co. Kildare, Ireland*
[3]*National Human Genome Research Institute, Bethesda, MD 20892, USA*
**Corresponding author: Peter J. M. van Haastert, p.j.m.van.haastert@rug.nl*

Phosphoinositides are involved in endocytosis in both mammalian cells and the amoeba *Dictyostelium discoideum*. Dd5P4 is the *Dictyostelium* homolog of human OCRL (oculocerebrorenal syndrome of Lowe); both have a RhoGAP domain and a 5-phosphatase domain that acts on phosphatidylinositol 4,5-bisphosphate/phosphatidylinositol 3,4,5-trisphosphate ($PI(3,4,5)P_3$). Inactivation of Dd5P4 inhibits growth on liquid medium and on bacteria. *Dd5p4*-null cells are impaired in phagocytosis of yeast cells. In wild-type cells, $PI(3,4,5)P_3$ is formed and converted to $PI(3,4)P_2$ just before closure of the phagocytic cup. In *dd5p4*-null cells, a phagocytic cup is formed upon contact with the yeast cell, and $PI(3,4,5)P_3$ is still produced, but the phagocytic cup does not close. We suggest that Dd5P4 regulates the conversion of $PI(3,4,5)P_3$ to $PI(3,4)P_2$ and that this conversion is essential for closure of the phagocytic cup. Phylogenetic analysis of OCRL-like 5-phosphatases with RhoGAP domains reveal that *D. discoideum* Dd5P4 is a surprisingly close homolog of human OCRL, the protein responsible for Lowe syndrome. We expressed human OCRL in *dd5p4*-null cells. Growth on bacteria and axenic medium is largely restored, whereas the rate of phagocytosis of yeast cells is partly restored, indicating that human OCRL can functionally replace *Dictyostelium* Dd5P4.

Key words: OCRL, phagocytosis, 5-phosphatase, phosphoinositide, pinocytosis

Received 14 February 2006, revised and accepted 29 January 2007

Many processes, including vesicle trafficking, are regulated by phosphoinositides (1,2). Binding of phosphoinositides to protein domains like pleckstrin homology (PH) domains and FYVE domains targets proteins to specific parts of the membrane. Proper signal transduction by phosphoinositides requires a tight control of their local concentrations. The formation of clathrin-coated vesicles and phagocytic cups is accompanied by the localized production of phosphatidylinositol 4,5-bisphosphate ($PI(4,5)P_2$) and phosphatidylinositol 3,4,5-trisphosphate ($PI(3,4,5)P_3$), respectively (3,4). One group of enzymes regulating the formation and degradation of phosphoinositides are inositol 5-phosphatases [reviewed by Erneux et al. (5)]. These enzymes remove the phosphate group from the 5-position of the inositol ring. The mammalian inositol 5-phosphatase SHIP (SRC Homology 2 Domain-containing Inositol-5-Phosphatase) is recruited to the membrane of the phagocytic cup, and negatively regulates phagocytosis (6). The inositol 5-phosphatase synaptojanin regulates vesicle recycling in the synapse (7). A role in vesicle trafficking is also proposed for the inositol 5-phosphatase OCRL (oculocerebrorenal syndrome of Lowe) (8). This protein contains a catalytic inositol 5-phosphatase domain and a C-terminal RhoGAP domain and localizes to *trans* Golgi network (TGN) in fibroblasts (8), consistent with a role of OCRL in lysosomal enzyme trafficking from the TGN to lysosomes (9). More recently, it has been demonstrated that OCRL protein associates with clathrin, localizes to endosomes and is proposed to play a role in clathrin-mediated trafficking of proteins from endosomes to the TGN (10,11). Mutations in the gene coding for OCRL results in the oculocerebrorenal syndrome of Lowe, affecting functions of the lens, kidney and nervous system (12). At a molecular level, elevated levels of $PI(4,5)P_2$ are observed (13,14) and the amount of long actin stress fibers in fibroblasts is decreased (15).

As in mammalian cell lines, phosphoinositides are also involved in endocytosis in the social amoeba *Dictyostelium discoideum* [reviewed in (16)]. Their natural food source, bacteria, are ingested via phagocytosis and the commonly used strain AX3 grows axenically by means of macropinocytosis. Inhibitors of the enzyme phospholipase C (PLC), which converts $PI(4,5)P_2$ into inositol 1,4,5-trisphosphate and diacylglycerol, drastically reduce the rate of phagocytosis (17). However, inactivation of the gene encoding the single *D. discoideum* $PI(4,5)P_2$–PLC does not affect growth (18). This suggests that the cells can switch to a PLC-independent pathway. Inactivation of the $PI(3,4,5)P_3$ producing phosphatidylinositol 3-kinases (PI3Ks) DdPIK1 and DdPIK2 decreases the rate of pinocytosis; however, phagocytosis is only slightly inhibited (19). On the other hand, both pinocytosis and growth on *Klebsiella aerogens* are inhibited by inactivation of the inositol 3-phosphatase PTEN (Phosphatase and Tensin-Homolog) (20). Five inositol 5-phosphatases, Dd5P1–4 and PLIP (phospholipid-inositol phosphatase), have been identified in *D. discoideum* (21,22). Dd5P1–4 are inositol 5-phosphatases containing the conserved motifs I and II (WXGDXN(Y/F)R and

P(A/S)W(C/T)DR(I/V)L) that are characteristic for inositol 5-phosphatases. The catalytic domain of Dd5P1 shows the highest similarity with SHIP, but lacks the N-terminal SH2 domain. A unique domain composition is present in Dd5P2 containing a 5-phosphatase and a RCC1-like domain. Dd5P3 and Dd5P4 have a domain composition similar to synaptojanin with a Sac1 domain, and to OCRL with a RhoGAP domain, respectively (Figure 1A). PLIP is not a classical inositol 5-phosphatase, as it does not contain the conserved motifs I and II. In stead, the amino acid sequence shows highest similarity with the inositol 3-phosphatase PTEN, although the preferred *in vitro* substrate is PI(5)P.

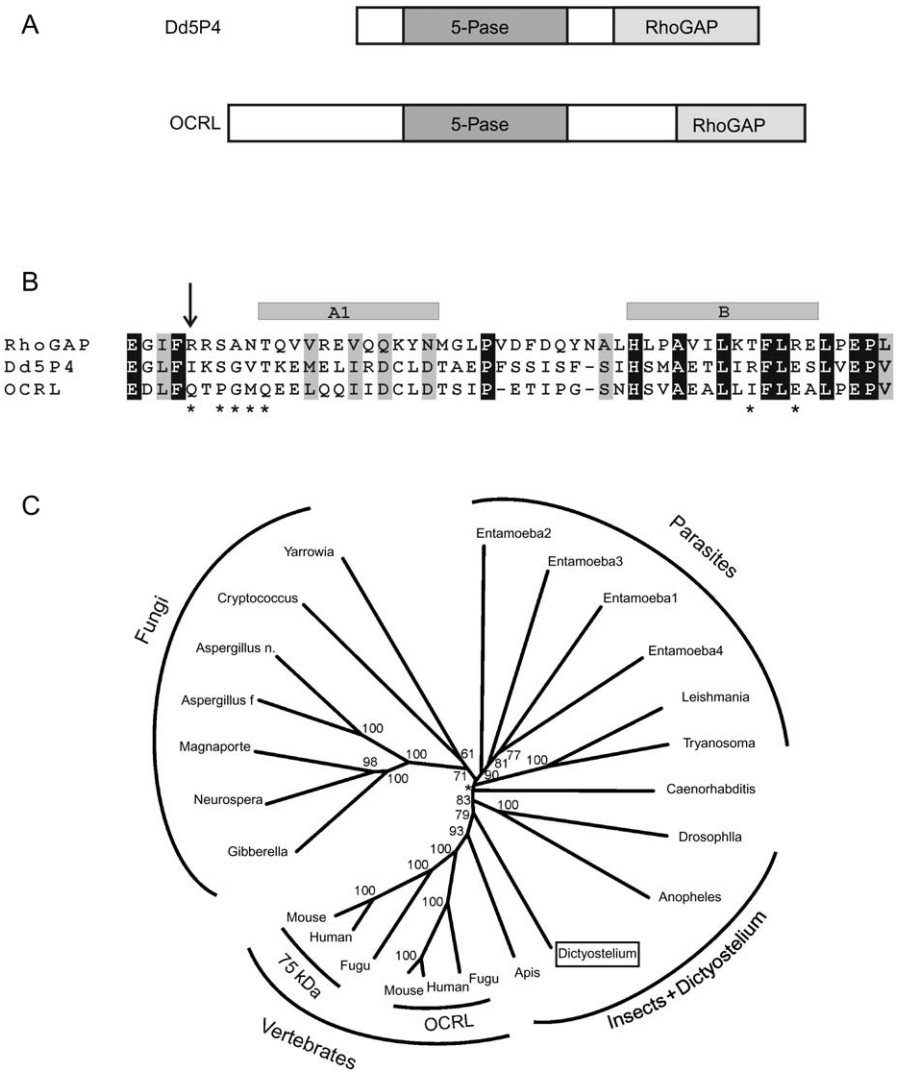

Figure 1: Protein domain composition and alignment of Dd5P4 and OCRL, and phylogeny of the OCRL family. A) Domain composition of *Dictyostelium discoideum* Dd5P4 and human OCRL. The abbreviation 5-Pase stands for inositol 5-phosphatase catalytic domain. B) Amino acids conserved between the RhoGAP domains of human RhoGAP, *D. discoideum* Dd5P4 and human OCRL are shown in black (100% identity) or gray (100% similarity). Asterisks indicate amino acids that interact with a small G protein as suggested by the crystal structure of RhoGAP in complex with RhoA. The arrow indicates the catalytic arginine present in the protein RhoGAP but absent in Dd5P4 and OCRL. C) Phylogeny of the OCRL family. Proteins that harbor both an inositol 5-phosphatase catalytic domain and a RhoGAP domain were identified from protein databases. The tree was built using CLUSTALW sequence alignment and PHYLIP (for the alignment we used the entire sequences from the beginning of the 5-phosphatase domain till the last amino acid, see *Materials and Methods* section). Numbers in the tree indicate bootstrap values in percent; the asterisk indicates bootstrap values below 50%. Species and GenBank entry numbers are: *Homo sapiens* (Human) OCRL, 67477390; *Mus musculus* (Mouse) OCRL, 46195807; *Takifugu rubripes* (Fugu) OCRL, SINFRUP00000157508; *H. sapiens* (Human) 75 kDa, 55665969; *M. musculus* (Mouse) 115 k[t1] , 7513696; *T. rubripes* (Fugu) 75 k, SINFRUP00000153548; *Apis mellifera* (honeybee), 66521204; *D. discoideum*, 60475249; *Anopheles gambiae*, 57924096; *Drosophila melanogaster*, 2749755; *Caenorhabditis elegans*, 3874363; *Trypanosoma brucei*, 70831128; *Leishmania major*, 68125488; *Entamoeba histolytica*, 67482035 (1), 67470251 (2), 56468394 (3), 67467066 (4); *Gibberella zeae*, 42546878; *Neurospora crassa*, 18376182; *Magnaporthe grisea*, 38108761; *Aspergillus fumigatus*, 66851486; *Aspergillus nidulans*, 40742343; *Cryptococcus neoformans*, 50255557; *Yarrowia lipolytica*, 49646035.

Inactivation of *dd5p1*, *dd5p2*, *dd5p3* or PLIP does not affect growth or development. In contrast, inactivation of *dd5p4* reduces axenic growth and inhibits growth on *K. aerogens*, suggesting a function for Dd5P4 in endocytosis (21).

In this report, we investigated the role of Dd5P4 during phagocytosis and showed that Dd5P4 is essential for this process. Mutational analysis shows that the inositol 5-phosphatase catalytic domain of Dd5P4 is essential for complementation of the *dd5p4*-null cells. Transfection of *dd5p4*-null cells with a truncated Dd5P4 lacking the C-terminal RhoGAP domain does not restore endocytic defects, suggesting that the C-terminal RhoGAP domain is essential as well (21). We expressed the human homolog OCRL in *D. discoideum dd5p4*-null cells and showed that expression of OCRL largely restores phagocytosis, growth and developmental defects of *dd5p4*-null cells.

The requirement for a functional inositol 5-phosphatase catalytic domain suggests that Dd5P4 regulates endocytosis by conversion of phosphoinositides. Recent data (23) have shown that PI(3,4,5)P_3 is formed in the early phagocytic cup upon contact of the particle, whereas PI(3,4)P_2 is formed later, shortly before and during cup closure. Based on our results in *dd5p4*-null cells with the PI(3,4)P_2/PI(3,4,5)P_3 reporter PH domain of cytosolic regulator of adenyl cyclase coupled to green fluorescent protein (PHcrac-GFP), we suggest that Dd5P4 mediates the conversion of PI(3,4,5)P_3 to PI(3,4)P_2 at the phagocytic cup, which is necessary for completion of the phagocytic process.

Results

Phylogeny of Dd5P4 and other OCRL-related proteins

Both *D. discoideum* Dd5P4 and human OCRL consist of an N-terminal 5-phosphatase domain and a C-terminal RhoGAP domain. We searched for the presence of the combination of these two domains in other proteins; databases were searched with BLAST, while domains were analyzed with SMART (see *Materials and Methods* section). The combination of an inositol 5-phosphatase domain and a RhoGAP domain is not observed in prokaryotes and only in a limited number of eukaryote species (Figure 1). Protein sequence alignment and the SMART domain scores reveal a well-defined 5-phosphatase domain in all these proteins, and a less well-defined RhoGAP domain. The RhoGAP domain has high SMART scores ($<1 \times 10^{-33}$) in the proteins present in metazoan and *D. discoideum*, intermediate SMART scores for parasites *Leishmania major*, *Trypanosoma brucei* and *Entamoeba histolytica* (about 1×10^{-5}) and detectable but insignificant scores for fungi ($>1 \times 10^{-1}$). Interestingly, the ~150 amino acid protein segment between the 5-phosphatase and RhoGAP domain shows rather good alignment.

Phylogenetic analysis of the OCRL family of proteins reveals that vertebrates contain two isoforms, OCRL and the 75-kDa type II 5-phosphatase. Insects, nematodes, *D. discoideum* and parasites contain only one gene, suggesting that the two isoforms in vertebrates evolved by relatively recent gene duplication. *Entamoeba histolytica*, a single-celled eukaryote parasite, contains four OCRL-like sequences that are not very homologous, suggesting that they are the result of early duplications in the lineage to *Entamoeba*. OCRL-like proteins are found in many fungi, but not in the yeast strains *Saccharomyces cerevisiae* and *Schizosaccharomyces pombe*. Also plants do not contain OCRL-like proteins with a 5-phosphatase and RhoGAP domain.

The position of the *D. discoideum* protein Dd5P4 relative to the proteins of other species is rather unexpected. It has been well established using phylogeny of many proteins that *D. discoideum* species evolved after plants, but before the fungi, and certainly far before *Caenorhabditis elegans* and *Drosophila melanogaster*. Nevertheless, the *D. discoideum* OCRL-like protein groups closer to vertebrate OCRL than the proteins from *C. elegans*, *D. melanogaster* and fungi. This close relationship is because of the good homology between human and *D. discoideum* protein over the entire sequence, especially the less-conserved RhoGAP domain. Therefore, *D. discoideum* protein Dd5P4 may represent a good candidate to study the function of human OCRL.

Inactivation of Dd5P4 inhibits macropinocytosis and phagocytosis

The commonly used *D. discoideum* strain AX3 grows both axenically and on bacterial lawns by means of macropinocytosis and phagocytosis, respectively. Inactivation of the gene coding for inositol 5-phosphatase Dd5P4 reduces growth rates in axenic medium and on bacterial lawns to $32 \pm 3\%$ and $22 \pm 8\%$, respectively (21, Table 1). The doubling time of wild-type cells with control plasmid is 15.7 ± 1.2 h, and increased drastically to 48.1 ± 3.6 h in *dd5p4*-null cells. When plated in association with *K. aerogens* as food source, wild-type AX3 cells form visible plaques after 3 days with a plating efficiency of $48 \pm 2\%$. In this assay, only $10.3 \pm 0.6\%$ of *dd5p4*-null cells form plaques. In addition, the plaques of *dd5p4*-null cells increased in size at approximately 1/5th the rate of wild-type AX3 cells (Table 1). To directly measure phagocytosis, we labeled heat-killed yeast cells with TRITC (Tetramethyl Rhodamine Iso-Thiocyanate) and measured uptake of these yeast particles by *D. discoideum*. Wild-type AX3 ingested about 1.5 yeast particles per hour per cell. Inactivation of Dd5P4 almost completely inhibited phagocytosis to about 4% of wild-type AX3 cells (Figure 2A; see also Figure 6B and Table 1).

Proteins are easily expressed in *D. discoideum* by placing the gene under the *D. discoideum* actin 15 promotor, transfecting the cells and selecting for transfected cells with G418. The actin 15 promotor ensures expression in the vegetative state as well as during development.

Table 1: Doubling time and rate of phagocytosis of used cell lines

Parental strain	Plasmid	Growth in axenic medium (% of control)	Phagocytosis (% of control)		
			Growth on bacteria		Yeast uptake
			Plating efficiency	Plaque growth	
AX3	Control plasmid	100 (def)	100 (def)	100 (def)	100 (def)
	Dd5P4-GFP	98 ± 10	116 ± 3*	120 ± 22*	133 ± 7*
	Dd5P4^{D319A}-GFP	79 ± 9*	98 ± 4	89 ± 12*	90 ± 3*
	OCRL	94 ± 9	100 ± 7	105 ± 16	ND
	OCRL^{D422A}	102 ± 9	96 ± 6	97 ± 14	ND
Dd5p4$^-$	None	32 ± 3*	21 ± 1*	22 ± 8*	3.7 ± 1.7*
	Control plasmid	34 ± 5*	22 ± 4*	20 ± 8*	ND
	Dd5P4-GFP	95 ± 10	84 ± 4*	95 ± 16	141 ± 16*
	Dd5P4	107 ± 8	99 ± 2	116 ± 17*	ND
	Dd5P4^{D319A}-GFP	31 ± 3*	18 ± 2*	26 ± 7*	0 ± 3*
	Dd5P4$^{\Delta RhoGAP}$	37 ± 4*	17 ± 1*	28 ± 8*	ND
	OCRL	84 ± 9*	65 ± 4*	59 ± 23*	22.6 ± 4.8*
	OCRL^{D422A}	31 ± 3*	22 ± 2*	27 ± 6*	ND

For growth in axenic medium, we determined the doubling time of each cell line. The results shown are the doubling time of AX3 with control plasmid (15.7 ± 1.2 h; mean ± standard deviation, $n = 6$) divided by the doubling time of the mutant. The doubling time of AX3 without vector is 12.6 ± 0.6 h. For growth on bacteria, we plated 250 or 1000 cells on solid medium in association with *Klebsiella aerogens*. After 3 and 4 days, the number and size of the colonies was determined. Shown are the plating efficiency of the mutant strain divided by the plating efficiency of AX3 with control plasmid (48 ± 2%; $n = 4$), and the plaque size of the mutant strain divided by the plaque size of AX3 with control plasmid on day 3 (2.5 ± 1.1 mm; $n = 16$). For phagocytosis of yeast cells, we measured the uptake of fluorescent yeast particles, expressed as a percentage of the rate of yeast uptake of AX3 with control plasmid (1.51 ± 0.08 yeast cells per *Dictyostelium discoideum* cell per hour; $n = 3$). ND, not determined. An asterisk indicates a significant difference to AX3 with control plasmid ($p < 0.01$).

Expression of Dd5P4-GFP, a protein in which GFP is C-terminally fused to Dd5P4, in *dd5p4*-null cells restored the defects in phagocytosis of yeast cells and growth on bacteria as well as growth in axenic medium (Figure 2A, Table 1). In fact, the rate of yeast phagocytosis (but not growth on bacteria or in axenic medium) by *dd5p4*$^-$/Dd5P4-GFP cells exceeded the rate of phagocytosis of wild-type AX3 cells to 141% of wild type. Overexpression of Dd5P4-GFP in wild-type cells also increased phagocytosis of yeast cells to 133% of wild type (Figure 2A, Table 1).

Expression of Dd5P4-GFP allows for the study of the localization of Dd5P4. In both vegetative and starved cells, Dd5P4-GFP was localized in the cytosol. We could not observe any localization to internal structures or the plasma membrane. Although the cells formed macropinocytic cups, no localization to the cups or endosomes was observed. Also no membrane localization of Dd5P4-GFP was observed in cells during phagocytosis of yeast particles (Figure 3).

The catalytic domain and the RhoGAP domain are essential for Dd5P4 function

Two conserved motifs, WXGDXN(Y/F)R and P(A/S)W(C/T)DR(I/V)L, are characteristic for inositol 5-phosphatases. Based on the crystal structure of the 5-phosphatase

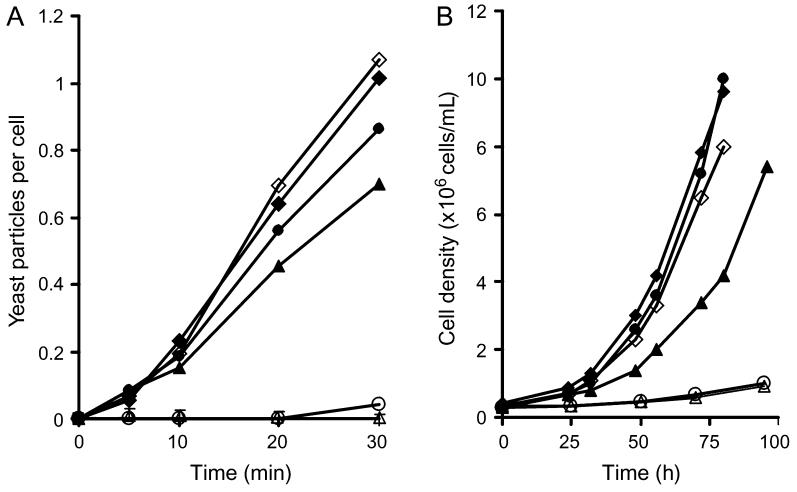

Figure 2: Axenic growth and phagocytosis of Dd5P4 mutants. Shown is the average of three experiments for yeast cell internalization (A) and a representative of the growth curves in axenic medium (B) of AX3 (closed circles), AX3/Dd5P4-GFP (closed diamonds), AX3/Dd5P4^{D319A}-GFP (closed triangle), *dd5p4*$^-$ (open circles), *dd5p4*$^-$/Dd5P4 (open diamonds) and *dd5p4*$^-$/Dd5P4^{D319A}-GFP (open triangles).

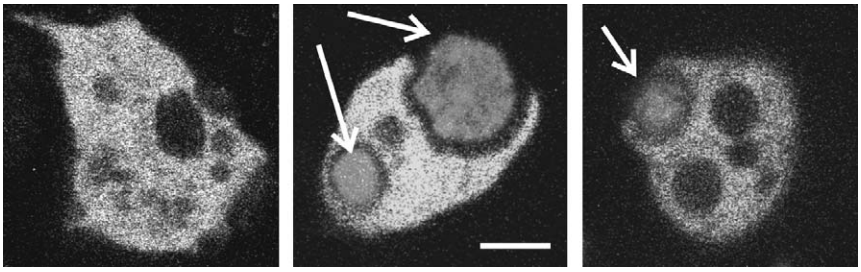

Figure 3: Localization of Dd5P4. *Dd5p4*-null cells were transfected with Dd5P4-GFP and analyzed by confocal microscopy. A vegetative cell is depicted in the left panel and cells ingesting yeast particles in the middle and right panel. The solid arrows indicate the yeast particles. The bar is 3 μm.

catalytic domain of SPsynaptojanin (Schizosaccharomyces pombe Synaptojanin), the aspartate present in the first motif was implicated to act as the catalytic base in the dephosphorylation reaction (24). This is supported by the fact that replacement of this aspartate by an alanine in the human platelet 75-kDa inositol polyphosphate 5-phosphatase II renders a 5-phosphatase inactive version of the protein (25). We mutated the corresponding aspartate in Dd5P4-GFP, Asp319, to an alanine and expressed the protein (Dd5P4^{D319A}-GFP) in a *dd5p4*-null background. Confocal fluoresence microscopy reveals that Dd5P4^{D319A}-GFP shows the same cytosolic localization as Dd5P4-GFP, both in a wild-type and in a *dd5p4*-null background (see Figure S1), implicating that the mutated protein was expressed at approximately equal levels as the wild-type protein. The growth rate in axenic medium (Figure 2B) or on bacterial lawn (Table 1) was not significantly restored in *dd5p4*$^-$/Dd5P4^{D319A}-GFP cells compared to *dd5p4*$^-$ cells (Figure 2B, Table 1). Uptake of yeast particles by *dd5p4*$^-$/Dd5P4^{D319A}-GFP cells was below detection levels, which is significantly lower than the uptake by *dd5p4*$^-$ cells (Figure 2A, Table 1). Overexpression of this catalytic inactive 5-phosphatase in wild-type cells (AX3/Dd5P4^{D319A}-GFP) lead to a statistically significant reduction of axenic growth by 21%, growth on bacteria by 11% and phagocytosis of yeast cells by 10% (Table 1). This inhibition could be due to competition of endogenously expressed wild-type Dd5P4 with the exogenously expressed catalytic inactive Dd5P4^{D319A}-GFP.

Dd5P4 contains a 5-phosphatase and a RhoGAP domain. We expressed a deletion mutant containing the active catalytic domain (21), but not the RhoGAP domain. These *dd5p4*$^-$/Dd5P4$^{\Delta RhoGAP}$ cells exhibited similar growth rates as *dd5p4*$^-$ cells, both in axenic medium and on bacteria, suggesting that an active catalytic domain is not sufficient to complement the *dd5p4*$^-$ cells. These studies implicate the necessity of both the inositol 5-phosphatase catalytic domain and the RhoGAP domain to restore growth defects.

We also expressed Dd5P4 without GFP tag in *dd5p4*-null cells because the C-terminal GFP tag may interfere with the function of the essential RhoGAP domain. We observed that Dd5P4 complemented *dd5p4*$^-$ cells slightly better than Dd5P4-GFP. The 10–20% faster growth in axenic medium and on bacteria is statistically significant.

The PH domain of CRAC localizes to the phagocytic and pinocytic cup in dd5p4-*null cells*

As phagocytosis is almost completely blocked in *dd5p4*-null cells, we wondered at which step of particle internalization the process was inhibited. The PI(3,4)P_2/PI(3,4,5)P_3 reporter protein PHcrac-GFP localizes to the phagocytic cup (23,26). We studied PHcrac-GFP localization in wild-type and *dd5p4*-null cells by confocal microscopy. The use of yeast particles labeled with TRITC allowed the detection of both PHcrac-GFP and the yeast cell. Images are presented in Figure 4 and quantitative data in Figure 5. In wild-type cells, contact of the cell with a yeast particle frequently triggered the formation of a PHcrac-GFP patch. This patch is restricted to the area of contact and increases in size upon extension of the phagocytic cup [(23,26), Figure 4A,B). Subsequently, the particle was engulfed and PHcrac-GFP dissociated from the membrane surrounding the particle within 1 min after internalization. On average, we observed approximately one phagocytic attempt per 10 min, which all resulted in a successful uptake of the yeast particle (Figure 5A). In *dd5p4*-null cells, interaction of the yeast particle with membrane components of the cell triggered the formation of a PHcrac-GFP patch as in wild-type cells (Figure 4C). The patch was located at the area in contact with the yeast cell and the intensity of the PHcrac-GFP patch was not drastically changed compared to wild-type cells. In addition, the frequency of interaction of *dd5p4*-null cells with yeast particles was approximately identical to that of wild-type cells (Figure 5A). However, these attempts were rarely successful, and we did not observe *dd5p4*-null cells in which the membrane extended beyond half of the yeast particle. In general, the membrane extensions of the phagocytic cup were withdrawn, the PHcrac-GFP patch disappeared and the yeast particle was subsequently released. In the rare case that we did observe an internalized yeast particle, some of these yeast particles were still labeled with PHcrac-GFP (Figure 4D). As a consequence, after 30 min of incubation with yeast particles, *dd5p4*-null cells contain only 0.06 ± 0.23 yeast particles/cell, compared to 0.96 ± 0.17 yeast particles/cell in wild-type AX3 cells. We conclude that *dd5p4*-null cells effectively recognize, bind and respond to yeast particles with enhanced PHcrac-GFP localization in the phagocytic cup, but that the phagocytic process is not completed.

We also used the PI(3,4)P_2 reporter TAPP1-PH-GFP in order to detect PI(3,4)P_2 specifically. As observed by

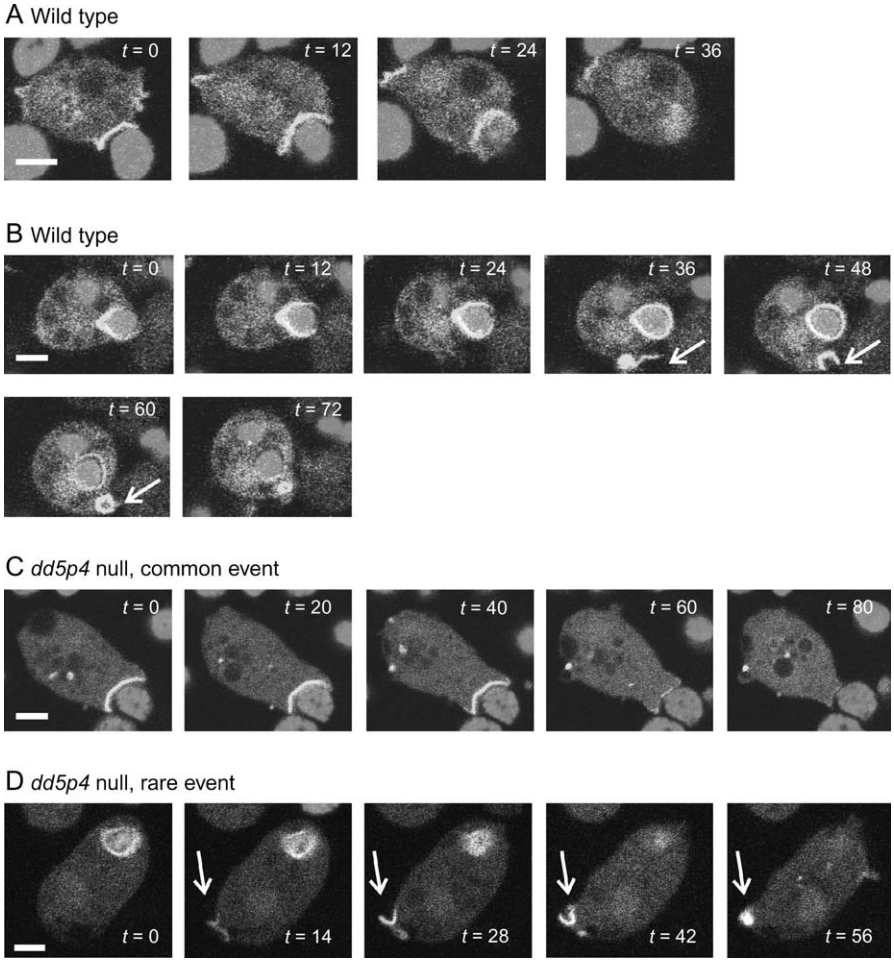

Figure 4: Localization of PHcrac-GFP in AX3 and *dd5p4*$^-$ cells during endocytosis. AX3 cells transfected with PHcrac-GFP (A,B) and *dd5p4*-null cells transfected with PHcrac-GFP (C,D) were incubated with TRITC-labeled yeast particles and analyzed by confocal microscopy. The time indicated in the corner of the picture is the time in seconds. Arrows point to the formation of a pinocytic cup. In panel C, the initial phagocytic cup is labeled with PHcrac-GFP, which is a common event for wild-type and *dd5p4*-null cells, but the yeast cell is not engulfed by the *dd5p4*-null cells. In panel D, the membrane surrounding an internalized yeast cell is labeled with PHcrac-GFP in the first frames before the yeast cell moves out of the confocal plane. Internalized yeast cells as shown in panel D are common for wild-type cells, but rarely observed in *dd5p4*-null cells (see also Figure 5). The bar is 3 μm.

Dormann et al. (23), in wild-type cells TAPP1-PH-GFP was not yet present at the membrane in the first steps of phagocytosis, but was detected just before cup closure. Unfortunately, we have been unable to transform the *dd5p4*-null cell line with the TAPP1-PH expression vector to investigate the formation of PI(3,4)P_2 during pinocytosis and phagocytosis. In three independent experiments, we observed small clones of cells resistant to the selection

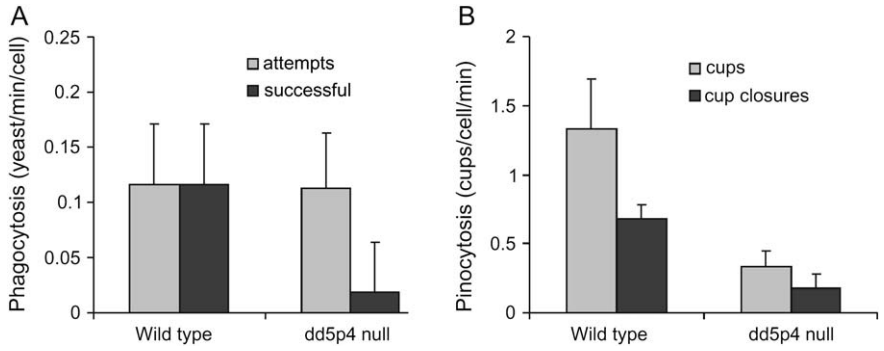

Figure 5: Formation and closure of phagocytic and pinocytic cups. AX3 cells and *dd5p4*-null cells transfected with PHcrac-GFP were incubated for about 30 min with TRITC-labeled yeast particles, and analyzed by confocal microscopy for 2 min as in Figure 4. For phagocytosis (A), we determined the number of events per minute of cells that made contact with a yeast particle and exhibited enhanced localization of PHcrac-GFP at the site of interaction, which is defined as attempts. In successful attempts, the yeast particle is engulfed. For pinocytosis (B), we determined the number of pinocytic cups stained with PHcrac-GFP per cell per minute, and the number of closed pinocytic cups visible as vesicles.

marker, but cells died when the clones contained between 10 and 20 cells, suggesting that expression of TAPP1-PH-GFP in *dd5p4*-null cell is lethal.

PHcrac-GFP patches are not only induced upon binding of yeast particles but are also formed at the membrane at apparently random places. In most cases, a pinocytic cup is formed at these positions and liquid is internalized. Localization of PHcrac-GFP to the endosome is visible up to 1 min after internalization. In the *dd5p4*-null cells, we observed similar structures as in wild-type cells with PHcrac-GFP patches, pinocytic cups and closed macropinosomes (Figure 4B,D). However, the frequency at which these structures appear are much lower in *dd5p4*-null cells (0.33 pinocytic cup/cell/min) than in wild-type cells (1.33 pinocytic cup/cell/min). For wild-type cells, we observed that approximately half of the pinocytic cups closed, yielding a macropinosome visible in the confocal plane, which was also observed in *dd5p4*-null cells (Figure 5B). We conclude that pinocytic cups labeled with PHcrac-GFP were formed at a reduced rates in *dd5p4*-null cells, but that subsequent cup closure and PHcrac-GFP localization to endosomes were not different from wild-type cells.

Expression of human OCRL largely rescues dd5p4*-null cells*

Sequence analysis of the inositol 5-phosphatase Dd5P4 has revealed the presence of a C-terminal RhoGAP domain (21). Human OCRL contains a C-terminal RhoGAP domain similar to Dd5P4 (Figure 1). Furthermore, both the inositol 5-phosphatase catalytic domain and RhoGAP domain of OCRL have a relatively high similarity with the corresponding domains of Dd5P4 (see above). Because of these similarities, we expressed human OCRL in *dd5p4*-null cells and analyzed the recovery in growth and phagocytosis. Expression of OCRL does restore axenic growth almost to the rate of wild-type cells, although the final cell density does not reach wild-type levels (Figure 6A, Table 1). When plated in association with *K. aerogens* as food source for 3 days, wild-type AX3 cells have formed plaques with a size of 2.5 ± 1.1 mm at a plating efficiency of $48 \pm 2\%$. In this assay, the plaques of *dd5p4*-null cells are only 0.5 ± 0.2 mm in size at a significantly lower plating efficiency of $10.3 \pm 0.6\%$. The *dd5p4*$^-$/OCRL cells exhibit a plaque size of 1.5 ± 0.5 mm and plating efficiency of $30 \pm 2\%$ that are intermediate between *dd5p4*$^-$ cells and wild-type cells. We also tested the uptake of yeast cells. Whereas the rate of yeast uptake for *dd5p4*-null cells is about 4% of wild-type AX3 cells, the rate of phagocytosis of *dd5p4*-null cells expressing OCRL is increased about fivefold to 23% of wild-type cells (Figure 6B, Table 1). Expression of OCRL^{D422A} with a mutation of the catalytic aspartate does not restore growth on bacteria or in axenic medium, indicating that OCRL, as Dd5P4, must be catalytically active to support growth.

Upon starvation, *D. discoideum* cells form multicellular aggregates. A single tip is formed at the top of the aggregate, and organizes the development into a multicellular slug and eventually a fruiting body with spores. Starvation of *dd5p4*-null cells results in the formation of multiple-tipped aggregates and consequently small fruiting bodies (21). Expression of OCRL in *dd5p4*-null cells restores this defect; cells form normal aggregates, slugs and fruiting bodies (data not shown). The results reveal that human OCRL can replace Dd5P4: phagocytosis of yeast particles is partly restored, plating efficiency and growth on bacterial lawns is largely restored, whereas growth on axenic medium and multicellular development is nearly completely restored.

Discussion

In mammalian cell lines, endocytosis and vesicle trafficking are regulated by phosphoinositides. In *D. discoideum*, the commonly used PI(3,4)P_2/PI(3,4,5)P_3 reporter PHcrac-GFP

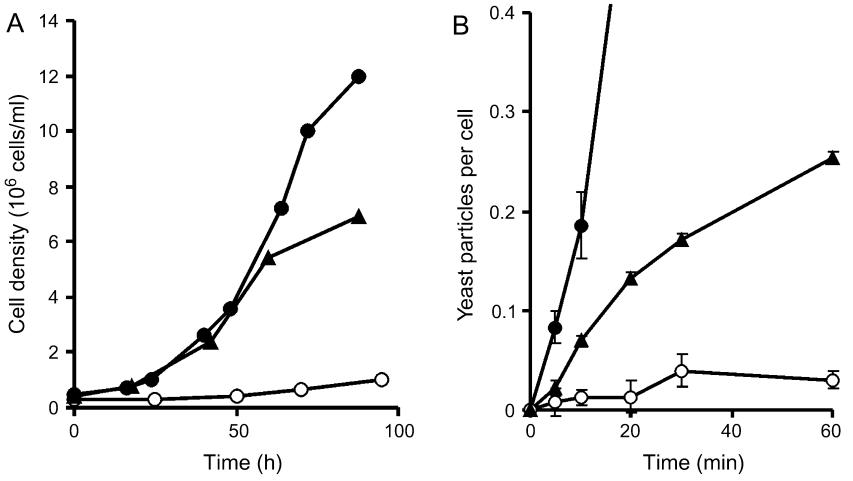

Figure 6: OCRL complements growth defects of *dd5p4*$^-$-null cells. Shown is a representative of the growth curves in axenic medium (A) and the average of three phagocytosis assays (B) of AX3 (closed circles), *dd5p4*$^-$ (open circles), *dd5p4*$^-$/OCRL (closed triangles).

is located at the pinocytic and phagocytic cup until about 1 min after internalization, suggesting a function for phosphoinositides in endocytosis of *D. discoideum* cells as well (23,26). Inactivation of two *D. discoideum* PI3Ks, DdPIK1 and DdPIK2, inhibits pinocytosis and inactivation of the 3-phosphatase PTEN inhibits growth on liquid medium and bacteria, supporting a function for phosphoinositides in pinocytosis and phagocytosis (20,27,28).

Function of inositol 5-phosphatase activity during endocytosis

Inactivation of the inositol 5-phosphatase *dd5p4* results in growth defects, indicating that Dd5P4 participates in endocytosis by regulating phosphoinositide levels (21). This is supported by data presented in this report showing that, in contrast to wild-type Dd5P4, the inositol 5-phosphatase inactive protein Dd5P4^{D319A}-GFP did not complement the growth defects of *dd5p4*-null cells, and even inhibited growth upon expression in wild-type cells. PI(4,5)P_2 and PI(3,4,5)P_3 are degraded *in vitro* by the catalytic domain of Dd5P4 (21). As PI(4,5)P_2 is the substrate for PI(3,4,5)P_3 production, reduced degradation of PI(4,5)P_2 or PI(3,4,5)P_3 *in vivo* could both lead to an increase of PI(3,4,5)P_3 levels.

Upon binding of a yeast cell, wild-type *D. discoideum* cells form a phagocytic cup. The sides of the cup extend along the yeast cell and eventually enclose the particle by fusion of the extending membranes. Yeast cells were still detected by the *dd5p4*-null cells at a normal frequency, and small phagocytic cups with membrane extension around the particles were formed as in wild-type cells. However, we rarely observed in *dd5p4*-null cells the further formation of cups that extended beyond half of the yeast cell or the subsequent fusion of extending membranes. As for wild-type cells, PHcrac-GFP localized to the membrane of *dd5p4*-null cells that was in contact with the yeast cell and the intensity of the PHcrac-GFP patch was not visibly altered if compared to wild type. This suggests that the total amount of PI(3,4)P_2/PI(3,4,5)P_3 was not drastically changed in *dd5p4*-null cells. As lack of inositol 5-phosphatase activity hampers phagocytosis, we suggest that the conversion of PI(3,4,5)P_3 to PI(3,4)P_2 is necessary for extension and closure of the phagocytic cup.

Dormann et al. (23) reported on the identity of the phosphoinositides that are formed during pinocytosis and phagocytosis using PH-GFP fusions that are specific for PI(3,4,5)P_3 (GRP1-PH-GFP) or for PI(3,4)P_2 (TAPP1-PH-GFP); PHcrac-GFP detects both PI(3,4,5)P_3 and PI(3,4)P_2. It was shown that during phagocytosis, PI(3,4,5)P_3 is formed upon attachment of the particle to the cell, while PI(3,4)P_2 becomes detectable significantly later in the process, just before and during cup closure. Transformation of *dd5p4*-null cells with the TAPP1-PH expression vector yielded cells that died when the clones contained between 10 and 20 cells. Wild-type cells could be transformed with the TAPP1-PH vector, and we confirmed the observations of Dormann et al. (23). Although many technical explanations are possible for these negative results, we suspect that expression of the PH domain of TAPP1 in *dd5p4*-null cell is lethal; *dd5p4*-null cells grow very slowly because of the reduced conversion of PI(3,4,5)P_3 to PI(3,4)P_2 at the closure of the endocyctic cup, and binding of the residual PI(3,4)P_2 by the PH domain of TAPP1 may block endocytosis completely. The study by Dormann et al. (23) and our previous and present experiments strongly suggest that the *Dictyostelium* OCRL-like protein Dd5P4 is responsible for the conversion of PI(3,4,5)P_3 to PI(3,4)P_2 at the closure of the phagocyctic cup. In this way, Dd5P4 and PI(3,4)P_2 may act as a conditional timer for completion of phagocytosis. In the absence of functional Dd5P4, either because of inactivation of the inositol 5-phosphatase activity or deletion of the RhoGAP domain, phagocytosis stalls halfway and the particle is released.

Implications of the restored endocytic defects by OCRL

In this report, we show that human OCRL can partly complement *dd5p4*-null cells for the lack of Dd5P4. Phagocytosis of yeast cells, that is strongly inhibited in *dd5p4*-null cells, is restored partly by OCRL from 4 to 22%, whereas the milder growth defects of *dd5p4*-null cells are restored from 21 to 62% (growth on bacteria) and from 32 to 84% (growth in axenic medium). Mutation of the catalytic aspartate of Dd5P4 renders the protein inactive in complementing *dd5p4*-null cells. The corresponding catalytic mutation in OCRL does also not complement *dd5p4*-null cells, suggesting that OCRL exhibits 5-phosphatase activity in *D. discoideum*. Several mutations in the OCRL gene of patients with Lowe syndrome have been identified leading to reduced 5-phosphatase activity (13). Dd5P4 contains a C-terminal RhoGAP domain in addition to the inositol 5-phosphatase catalytic domain. This domain is not present in either one of the remaining inositol 5-phosphatases in *dd5p4*-null cells, the SHIP-like Dd5P1, the unique Dd5P2 and the synaptojanin-like Dd5P3. Transfection of *dd5p4*-null cells with an extrachromosomal plasmid only containing the catalytic domain of Dd5P4 does not restore any of the observed defects in *dd5p4*-null cells, including poor growth on bacteria. These observations strongly implicate an essential function for the RhoGAP domain, next to the 5-phosphatase domain, and also suggest the presence of a small G protein in *D. discoideum* cells that can bind both the RhoGAP domain of Dd5P4 and human OCRL.

The phylogenetic cluster analysis of OCRL-like proteins with inositol 5-phosphatase and RhoGAP domains reveals an unexpected close relationship between *Dictyostelium* OCRL-like Dd5P4 and vertebrate OCRL. Many OCRL-like proteins from lower eukaryotes have a poorly conserved RhoGAP domain. In contrast to other lower eukaryotes,

the RhoGAP domain of Dd5P4 has relatively high similarity with the RhoGAP domain of OCRL. In fact, the RhoGAP domain of Dd5P4 is more closely related to the RhoGAP domain of the human inositol 5-phosphatases OCRL than to other *D. discoideum* RhoGAP domains present in the data bank. *Saccharomyces cerevisiae* do not possess OCRL-like proteins with a RhoGAP domain, but three synaptojanin-like inositol 5-phosphatases and one inositol 5-phosphatase not containing another identified domain. Human OCRL-like 5-phosphatase II restores the phenotypic defects of null mutants of these inositol 5-phosphatases (29), suggesting that the 5-phosphatase activity of OCRL is sufficient for complementation in yeast. However, the necessity of a RhoGAP domain for Dd5P4 function in *D. discoideum* makes Dd5P4 a good candidate to serve as a model for human OCRL.

Recently, it has been reported that the RhoGAP domain of human OCRL binds to the small G protein Rac1 (30,31). For *D. discoideum*, human Rac1 is closely related to the *Dictyostelium* Rac1A-C family (unpublished data). Interestingly, it has been demonstrated that the Rac1 family of small G proteins is involved in endocytosis in *D. discoideum* (32). Human OCRL is localized to the TGN, but does not contain a membrane-targeting domain (8,12). As small G proteins are prenylated and thereby targeted to the membrane, binding of OCRL to Rac1 could mediate the localization of OCRL. Extrapolation of these data to *D. discoideum* would implicate a role for the RhoGAP domain in membrane localization and explain the requirement for a RhoGAP domain. However, as we could not observe membrane localization of Dd5P4 under the conditions tested, either the interaction with the small G protein is too transient, or the amounts of interacting proteins is too low or the RhoGAP domain does not function as a membrane-targeting domain in *D. discoideum*.

Expression of human OCRL in *dd5p4*-null cells restores the endocytic defects, but not to wild-type levels. This could be as a result of poor expression of human OCRL in *D. discoideum*, to less efficient binding of OCRL to the *D. discoideum* small G protein and/or to lower GTPase activating protein activity of OCRL compared to Dd5P4. The crystal structure of the human RhoGAP, which is homologous to the RhoGAP domain of Dd5P4 and OCRL, has been solved in complex with the small GTP-binding protein RhoA (33). This revealed a catalytic role for an arginine, $Arg85_{p50RhoGAP}$, located at the loop between helix A and A1. This loop, together with helix B and F, form most of the interactions between RhoGAP and RhoA. Many of the amino acids that interact with the small G protein, including the catalytic arginine, are not conserved in both Dd5P4 and OCRL (Figure 1). Furthermore, a number of these amino acids in Dd5P4 are also not similar to the corresponding amino acids in OCRL. This supports the idea that less efficient binding of the RhoGAP domain of OCRL to the *D. discoideum* small G protein may cause the partial rescue of phagocytosis.

Materials and Methods

Phylogeny of OCRL-related proteins

Genomic and protein databases were searched with BLAST (http://www.ncbi.nlm.nih.gov) for the presence of proteins containing both 5-phosphatase and RhoGAP domains. Initial searches were carried out with the complete open reading frame of human OCRL and *D. discoideum* Dd5P4, yielding sequences from metazoan, some parasites and some fungi. Domain architecture was analyzed with SMART (smart.embl-heidelberg.de), indicating very high scores for the 5-phosphatase domains (about 1×10^{-140} for metazoan, 1×10^{-123} for *D. discoideum* and 1×10^{-30} for parasites and fungi), but lower scores for the RhoGAP domain (about 1×10^{-40} for metazoan, 1×10^{-33} for *D. discoideum*, 1×10^{-5} for parasites and insignificant $1 \times 10^{+1}$ scores for fungi). Sequence alignment was performed by CLUSTALW analysis, revealing very good alignment of the 5-phosphatase domain and reasonable alignment of the RhoGAP domain, but also unexpected good alignment of the ~180 amino acids between the 5-phosphatase and RhoGAP domain. Therefore, databases were searched again with a C-terminal segment of the OCRL or Dd5P4 protein containing about 50 amino acids of the 5-phosphatase domain, the RhoGAP domain and the connecting domain, yielding several additional sequences in Entamoeba and fungi. These new sequences all had a RhoGAP domain with low scores in SMART. Finally, databases were searched with only the connecting domain. All proteins with significant BLAST scores contained both the 5-phosphatase and RhoGAP domain and were already found in the previous searches.

Phylogenetic analysis was performed with PHYLIP, using the alignment of the complete proteins, except the very variable section before the 5-phosphatase domain (thus the complete 5-phosphatase domain, RhoGAP domain and domain between 5-phosphatase and RhoGAP).

Strains and growth conditions

The *D. discoideum* strains AX3 (wild type), *dd5p4*-null and derivatives were grown in HG5 medium and supplemented with 10 μg/mL G418 when necessary. When grown in shaking culture, the cell density was kept between 5×10^5 and 6×10^6 cells/mL. To determine growth rate, doubling times were determined in the exponential phase of the growth curve. Growth and development on bacterial lawns was studied using *K. aerogens* grown on 3× LP plates (8.3 mM lactose, 2 mM KH_2PO_4, 2 mM Na_2HPO_4, 15 g/L agar). Unless stated otherwise, *D. discoideum* cells were grown and assayed at 22°C.

Expression of proteins in D. discoideum

To express proteins in *D. discoideum*, the desired genes were cloned behind the actin 15 promotor of the extrachromosomal plasmid MB74 or DM6. These plasmids contain a neomycin cassette, which allows selection with G418 for cells containing the plasmid. MB74 is a derivative of MB12neo, in which the terminator in the neomycin cassette has been replaced by one actin 8 terminator. DM6 is a derivative of MB74 also containing the gene coding for enhanced GFP. Previously (21), we described the cloning of full-length Dd5P4 and $Dd5P4^{\Delta RhoGAP}$ (with the name cat5P4). GFP fusion proteins of Dd5P4 were constructed by polymerase chain reaction (PCR) using a reverse primer lacking the stop codon and in frame fusion with the ''GFP open reading frame'' in DM6. To obtain a catalytic inactive mutant, the aspartate at position 319 was mutated into an alanine by site-directed mutagenesis, simultaneously introducing a *Sac*I restriction site by silent mutagenesis of Gly318 and Leu320.

Using PCR, the human OCRL was amplified from pTarget-OCRL and cloned into MB74, yielding plasmid pOCRL. Based on heterologous expression studies (34), we optimized the first 13 codons, using the forward primer OCRL-s1 (AATTAGGATCC **ATG** GAG CCA CCA CTC CCA GTC GGA GCC CAA CCA CTT GCC), to obtain proper expression of human OCRL in *D. discoideum*. To obtain a catalytic inactive mutant of OCRL, the aspartate at position 422 was mutated into an alanine by site-directed mutagenesis with plasmid pOCRL as target, simultaneously introducing a *Sac*I restriction

site by silent mutagenesis of Leu423. All gene fragments obtained by PCR were verified by sequencing.

Phagocytosis assay

Heat-killed yeast cells were fluorescently labeled with TRITC (1 mg/10^{10} yeast particles) and resuspended in phosphate buffer (PB) (10 mM Na_2HPO_4/KH_2PO_4, pH 6.5; 10^9 yeast particles/mL PB) (35). *Dictyostelium discoideum* cells were grown in shaking culture, collected and washed once with PB. Cells were resuspended (2×10^7 cells/mL PB) and transferred to glass tubes. Samples (112 μL) were taken after indicated times of incubation at 150 × ***g*** with labeled yeast particles (final concentration of 1.1×10^8 yeast particles/mL). Phagocytosis was stopped by addition of ice-cold PB (1 mL) and samples were kept on ice. After addition of 100 μL trypan blue (2 mg/mL in 20 mM citrate, 150 mM NaCl, pH 4.5) and incubation for 5 min at 200 × ***g***, cells were spun down (3 min at 500 × ***g***), resuspended in 1 mL PB and fluorescence was measured (excitation: 544 nm, emission: 574 nm).

Confocal images

To obtain confocal images of cells ingesting yeast, *D. discoideum* cells were washed with PB and TRITC-labeled yeast particles were added. To obtain confocal images of cells expressing PHcrac-GFP or TAPP1-PH-GFP, cells were transfected with plasmid WF38 (kind gift of P. N. Devreotes) or plasmid TAPP1-PH-GFP (kind gift of C. Weijer), respectively.

Images were obtained using a Zeiss LSM510 confocal fluorescence microscope (Carl Zeiss Jena, Germany) with a Plan-Apochromat × 63 magnification 1.40 aperture oil immersion objective. Using an argon laser, fluorescence of PHcrac-GFP and TRITC-yeast were determined at wavelengths 488 nm and 543 nm in combination with a 500–530 nm and 565–615 nm filter, respectively.

Acknowledgments

We thank Ineke Keizer, Arjen Krikken and Marten Veenhuis for their help in obtaining the confocal images, Peter Devreotes for plasmid WF38, Dirk Dormann and Kees Weijer for TAPP1-PH expression vector and Jeroen Hoeboer for his work on the *dd5p4*$^-$/OCRL cell line. This work was supported by The Netherlands Organization of Scientific Research.

Supplementary Material

Figure S1: Confocal fluorescent images of AX3 wild-type cells and dd5p4-null cells expressing Dd5P4-GFP or the catalytic inactive mutant Dd5P4D319A-GFP. The field of observation is 100 × 100 ×m.

Supplemental materials are available as part of the online article at http://www.blackwell-synergy.com

References

1. Corvera S, D'Arrigo A, Stenmark H. Phosphoinositides in membrane traffic. Curr Opin Cell Biol 1999;11:460–465.
2. Dyson JM, O'Malley CJ, Becanovic J, Munday AD, Berndt MC, Coghill ID, Nandurkar HH, Ooms LM, Mitchell CA. The SH2-containing inositol polyphosphate 5-phosphatase, SHIP-2, binds filamin and regulates submembraneous actin. J Cell Biol 2001;155:1065–1079.
3. Botelho RJ, Teruel M, Dierckman R, Anderson R, Wells A, York JD, Meyer T, Grinstein S. Localized biphasic changes in phosphatidylinositol-4,5-bisphosphate at sites of phagocytosis. J Cell Biol 2000;151:1353–1368.
4. Marshall JG, Booth JW, Stambolic V, Mak T, Balla T, Schreiber AD, Meyer T, Grinstein S. Restricted accumulation of phosphatidylinositol 3-kinase products in a plasmalemmal subdomain during Fc gamma receptor-mediated phagocytosis. J Cell Biol 2001;153:1369–1380.
5. Erneux C, Govaerts C, Communi D, Pesesse X. The diversity and possible functions of the inositol polyphosphate 5-phosphatases. Biochim Biophys Acta 1998;1436:185–199.
6. Cox D, Dale BM, Kashiwada M, Helgason CD, Greenberg S. A regulatory role for Src homology 2 domain-containing inositol 5'-phosphatase (SHIP) in phagocytosis mediated by Fc gamma receptors and complement receptor 3 (alpha(M)beta(2); CD11b/CD18). J Exp Med 2001;193:61–71.
7. Cremona O, Di Paolo G, Wenk MR, Luthi A, Kim WT, Takei K, Daniell L, Nemoto Y, Shears SB, Flavell RA, McCormick DA, De Camilli P. Essential role of phosphoinositide metabolism in synaptic vesicle recycling. Cell 1999;99:179–188.
8. Dressman MA, Olivos-Glander IM, Nussbaum RL, Suchy SF. Ocrl1, a PtdIns(4, 5)P(2) 5-phosphatase, is localized to the trans-Golgi network of fibroblasts and epithelial cells. J Histochem Cytochem 2000;48:179–190.
9. Ungewickell AJ, Majerus PW. Increased levels of plasma lysosomal enzymes in patients with Lowe syndrome. Proc Natl Acad Sci U S A 1999;96:13342–13344.
10. Ungewickell A, Ward ME, Ungewickell E, Majerus PW. The inositol polyphosphate 5-phosphatase Ocrl associates with endosomes that are partially coated with clathrin. Proc Natl Acad Sci U S A 2004;101:13501–13506.
11. Choudhury R, Diao A, Zhang F, Eisenberg E, Saint-Pol A, Williams C, Konstantakopoulos A, Lucocq J, Johannes L, Rabouille C, Greene LE, Lowe M. Lowe syndrome protein OCRL1 interacts with clathrin and regulates protein trafficking between endosomes and the trans-Golgi network. Mol Biol Cell 2005;16:3467–3479.
12. Suchy SF, Olivos-Glander IM, Nussbaum RL. Lowe syndrome, a deficiency of phosphatidylinositol 4,5-bisphosphate 5-phosphatase in the Golgi apparatus. Hum Mol Genet 1995;4:2245–2250.
13. Zhang X, Hartz PA, Philip E, Racusen LC, Majerus PW. Cell lines from kidney proximal tubules of a patient with Lowe syndrome lack OCRL inositol polyphosphate 5-phosphatase and accumulate phosphatidylinositol 4,5-bisphosphate. J Biol Chem 1998;273:1574–1582.
14. Wenk MR, Lucast L, Di Paolo G, Romanelli AJ, Suchy SF, Nussbaum RL, Cline GW, Shulman GI, McMurray W, De Camilli P. Phosphoinositide profiling in complex lipid mixtures using electrospray ionization mass spectrometry. Nat Biotechnol 2003;21:813–817.
15. Suchy SF, Nussbaum RL. The deficiency of PIP2 5-phosphatase in Lowe syndrome affects actin polymerization. Am J Hum Genet 2002;71:1420–1427.
16. Cardelli J. Phagocytosis and macropinocytosis in Dictyostelium: phosphoinositide-based processes, biochemically distinct. Traffic 2001;2:311–320.
17. Peracino B, Borleis J, Jin T, Westphal M, Schwartz JM, Wu L, Bracco E, Gerisch G, Devreotes P, Bozzaro S. G protein beta subunit-null mutants are impaired in phagocytosis and chemotaxis due to inappropriate regulation of the actin cytoskeleton. J Cell Biol 1998;141:1529–1537.
18. Drayer AL, Van der Kaay J, Mayr GW, Van Haastert PJM. Role of phospholipase C in Dictyostelium: formation of inositol 1,4,5-trisphosphate and normal development in cells lacking phospholipase C activity. EMBO J 1994;13:1601–1609.
19. Buczynski G, Grove B, Nomura A, Kleve M, Bush J, Firtel RA, Cardelli J. Inactivation of two Dictyostelium discoideum genes, DdPIK1 and DdPIK2, encoding proteins related to mammalian phosphatidylinositide 3-kinases, results in defects in endocytosis, lysosome to postlysosome transport, and actin cytoskeleton organization. J Cell Biol 1997;136:1271–1286.

20. Iijima M, Devreotes P. Tumor suppressor PTEN mediates sensing of chemoattractant gradients. Cell 2002;109:599–610.
21. Loovers HM, Veenstra K, Snippe H, Pesesse X, Erneux C, van Haastert PJM. A diverse family of inositol 5-phosphatases playing a role in growth and development in Dictyostelium discoideum. J Biol Chem 2003;278:5652–5658.
22. Merlot S, Meili R, Pagliarini DJ, Maehama T, Dixon JE, Firtel RA. A PTEN-related 5-phosphatidylinositol phosphatase localized in the Golgi. J Biol Chem 2003;278:39866–39873.
23. Dormann D, Weijer G, Dowler S, Weijer CS. In vivo analysis of 3-phosphoinositide dynamics during Dictyostelium phagocytosis and chemotaxis. J Cell Sci 2004;117:6497–6509.
24. Tsujishita Y, Guo S, Stolz LE, York JD, Hurley JH. Specificity determinants in phosphoinositide dephosphorylation: crystal structure of an archetypal inositol polyphosphate 5-phosphatase. Cell 2001;105: 379–389.
25. Jefferson AB, Majerus PW. Mutation of the conserved domains of two inositol polyphosphate 5-phosphatases. Biochemistry 1996;35: 7890–7894.
26. Devreotes P, Janetopoulos C. Eukaryotic chemotaxis: distinctions between directional sensing and polarization. J Biol Chem 2003;278: 20445–20448.
27. Zhou K, Pandol S, Bokoch G, Traynor-Kaplan AE. Disruption of Dictyostelium PI3K genes reduces [^{32}P]phosphatidylinositol 3, 4 bisphosphate and [^{32}P]phosphatidylinositol trisphosphate levels, alters F-actin distribution and impairs pinocytosis. J Cell Sci 1998;111: 283–294.
28. Funamoto S, Meili R, Lee S, Parry L, Firtel RA. Spatial and temporal regulation of 3-phosphoinositides by PI 3-kinase and PTEN mediates chemotaxis. Cell 2002;109:611–623.
29. O'Malley CJ, McColl BK, Kong AM, Ellis SL, Wijayaratnam AP, Sambrook J, Mitchell CA. Mammalian inositol polyphosphate 5-phosphatase II can compensate for the absence of all three yeast Sac1-like-domain-containing 5-phosphatases. Biochem J 2001;355:805–817.
30. Faucherre A, Desbois P, Satre V, Lunardi J, Dorseuil O, Gacon G. Lowe syndrome protein OCRL1 interacts with Rac GTPase in the trans-Golgi network. Hum Mol Genet 2003;12:2449–2456.
31. Faucherre A, Desbios P, Nagano F, Satre V, Lunardi J, Gacon G, Dorseuil O. Lowe syndrome protein Ocrl1 is translocated to membrane ruffles upon Rac GTPase activation: a new perspective on Lowe syndrome pathophysiology. Hum Mol Genet 2005;14:1441–1448.
32. Dumontier M, Hocht P, Mintert U, Faix J. Rac1 GTPases control filopodia formation, cell motility, endocytosis, cytokinesis and development in Dictyostelium. J Cell Sci 2000;113:2253–2265.
33. Rittinger K, Walker PA, Eccleston JF, Smerdon SJ, Gamblin SJ. Structure at 1.65 A of RhoA and its GTPase-activating protein in complex with a transition-state analogue. Nature 1997;389:758–762.
34. Vervoort EB, van Ravestein A, van Peij NNME, JC Heikoop, van Haastert PJM, Verheijden GF, Linskens MHK. Optimizing heterologous expression in dictyostelium: importance of 5′ codon adaptation. Nucleic Acids Res 2000;28:2069–2074.
35. Maniak M, Rauchenberger R, Albrecht R, Murphy J, Gerisch G. Coronin involved in phagocytosis: dynamics of particle-induced relocalization visualized by a green fluorescent protein Tag. Cell 1995;83:915–924.